

# Two-pion-exchange parity-violating potential and $np \rightarrow d\gamma$

C. H. Hyun<sup>1</sup>, S. Ando<sup>1</sup>, and B. Desplanques<sup>2</sup>

<sup>1</sup> Department of Physics and Institute of Basic Science, Sungkyunkwan University, Suwon 440-746, Korea

<sup>2</sup> Laboratoire de Physique Subatomique et de Cosmologie (UMR CNRS/IN2P3-UJF-INPG), F-38026 Grenoble Cedex, France

Received: date / Revised version: date

**Abstract.** We calculate the parity-violating nucleon-nucleon potential in heavy-baryon chiral perturbation theory up to the next-to-next-to-leading order. The one-pion exchange comes in the leading order and the next-to-next-to-leading order consists of two-pion-exchange and the two-nucleon contact terms. In order to investigate the effect of the higher order contributions, we calculate the parity-violating asymmetry in  $np \rightarrow d\gamma$  at the threshold. The one-pion dominates the physical observable and the two-pion contribution is about or less than 10% of the one-pion contribution.

**PACS.** 21.30.Fe Forces in hadronic systems and effective interactions – 12.15.Ji Applications of electroweak models to specific processes

## 1 Introduction

We employ the idea of effective field theory (EFT) to derive the parity-violating (PV) nucleon-nucleon ( $NN$ ) potential and apply it to the calculation of the PV photon asymmetry  $A_\gamma$  in  $np \rightarrow d\gamma$  at threshold. The PV  $NN$  potential is obtained by replacing a parity-conserving (PC) vertex in the strong  $NN$  potential with a PV vertex. Most of the low energy PV calculations have been relying on one-meson exchange potential, the so-called DDH potential [1]. Some literature investigated the PV two-pion-exchange potential (TPEP) in the past [2,3,4], and it was revived quite recently in the light of EFT [5]. In ref. [5], a thorough derivation of the PV potential is performed up to the next-to-next-to-leading order (NNLO) in both pionless and pionful EFTs. Since the PV asymmetry in  $np \rightarrow d\gamma$  is sensitive to the pion exchange contribution, we adopt heavy-baryon chiral perturbation (HB $\chi$ PT) and obtain the potential relevant to  $np \rightarrow d\gamma$  up to NNLO.

Theoretical estimations of  $A_\gamma$  have been extensively worked out with the DDH potential [6,7,8,9]. The results with various strong interaction models turn out basically identical.  $A_\gamma$  is dominated by the PV one-pion-exchange potential (OPEP) and the heavy-meson contribution is negligible. Thus it is discussed that the measurements of  $A_\gamma$  could provide us an opportunity to determine the weak pion-nucleon coupling constant  $h_\pi^1$ . On the other hand, possibility of a 10% effect from the PV TPEP has been discussed [10].

In this work we present the first estimation of the intermediate-range contribution to  $A_\gamma$ . We employ the Argonne v18 potential for the PC potential and the Siegert's theorem for the current operators. The PV potential relevant to  $np \rightarrow d\gamma$  in our study comprises OPEP and TPEP.

There are various terms other than the TPEP that appear at the NNLO: two-nucleon contact term, higher order correction of PC and PV  $\pi NN$  vertices, and etc. In the present work, we retain only the TPEP and neglect the remaining NNLO contributions for simplicity. The effect of the remaining terms will be considered elsewhere [11].

The NNLO calculation will allow us to estimate the order and the magnitude of higher order corrections, which will be important in pinning down the value of  $h_\pi^1$  and its uncertainty. At the same time, the NNLO contribution will provide a criterion for the validity of EFT approach to the PV phenomena.

## 2 Formalism

### 2.1 PV potential

The PV potential relevant to our estimation of  $A_\gamma$  in momentum space has the form

$$\tilde{V}_i(\mathbf{q}) = i(\boldsymbol{\tau}_1 \times \boldsymbol{\tau}_2)^z (\boldsymbol{\sigma}_1 + \boldsymbol{\sigma}_2) \cdot \mathbf{q} \tilde{v}_i(q), \quad (1)$$

where  $q \equiv |\mathbf{q}|$  and  $\mathbf{q} = \mathbf{p}_1 - \mathbf{p}_2$ . OPE and TPE terms are obtained as

$$\tilde{v}_{1\pi}(q) = -\frac{g_A h_\pi^1}{2\sqrt{2}f_\pi} \frac{1}{q^2 + m_\pi^2}, \quad (2)$$

$$\tilde{v}_{2\pi}(q) = \sqrt{2}\pi \frac{h_\pi^1}{A_\chi^3} \left\{ g_A \tilde{L}(q) - g_A^3 \left[ 3\tilde{L}(q) - \tilde{H}(q) \right] \right\}, \quad (3)$$

with

$$\tilde{L}(q) = \frac{\sqrt{q^2 + 4m_\pi^2}}{q} \ln \left( \frac{\sqrt{q^2 + 4m_\pi^2} + q}{2m_\pi} \right), \quad (4)$$

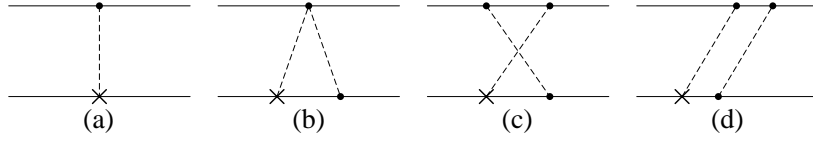


**Fig. 1.** Diagrams for PV OPE and TPE potentials. The diagram (a) is for the OPE term and the diagram (b-d) are for the TPE ones. Lines (dashed lines) denote nucleons (pions), vertices with a dot represent PC vertices, vertices with “ $\times$ ” represent the PV vertex proportional to  $h_\pi^1$ .

$$\tilde{H}(q) = \frac{4m_\pi^2}{q^2 + m_\pi^2} \tilde{L}(q), \quad (5)$$

where  $g_A$  is the axial coupling constant,  $f_\pi$  the pion decay constant and  $A_\chi = 4\pi f_\pi$ . The potential of eq. (1) in the coordinate space can be written as

$$V_i(\mathbf{r}) = \int \frac{d^3\mathbf{q}}{(2\pi)^3} \tilde{V}_i(\mathbf{q}) e^{-i\mathbf{q}\cdot\mathbf{r}} \\ = i(\boldsymbol{\tau}_1 \times \boldsymbol{\tau}_2)^z (\boldsymbol{\sigma}_1 + \boldsymbol{\sigma}_2) \cdot [\mathbf{p}, v_i(r)], \quad (6)$$

where  $\mathbf{p}$  is the conjugate momentum of the relative coordinate  $\mathbf{r} \equiv \mathbf{r}_1 - \mathbf{r}_2$ . For easier numerical calculation, we cast eqs. (4,5) into the dispersion relations as

$$\tilde{L}(q) = - \int_{4m_\pi^2}^{\infty} \frac{dt'}{2\sqrt{t'}} \sqrt{t' - 4m_\pi^2} \left( \frac{1}{t' + q^2} - \frac{1}{t' - 4m_\pi^2} \right), \quad (7)$$

$$\tilde{H}(q) = \frac{4m_\pi^2}{2} \int_{4m_\pi^2}^{\infty} \frac{dt'}{\sqrt{t'}} \frac{1}{\sqrt{t' - 4m_\pi^2}} \frac{1}{t' + q^2}. \quad (8)$$

Furthermore, we introduce a monopole form factor of the type  $\Lambda^2/(\Lambda^2 + q^2)$  in the Fourier transformation of eq. (1). The roles of the form factor and the cutoff are (i) to make the numerical calculation more easier and efficient, and (ii) to cut away high momentum region where the dynamics is essentially unknown and irrelevant to the low energy processes. With the form factor, we rewrite the potential in coordinate space as

$$V_i^A(\mathbf{r}) = i(\boldsymbol{\tau}_1 \times \boldsymbol{\tau}_2)^z (\boldsymbol{\sigma}_1 + \boldsymbol{\sigma}_2) \cdot [\mathbf{p}, v_i^A(r)] \quad (9)$$

where

$$v_{1\pi}^A = \frac{g_A h_\pi^1}{2\sqrt{2}f_\pi} \frac{\Lambda^2}{\Lambda^2 - m_\pi^2} \frac{1}{4\pi r} (e^{-m_\pi r} - e^{-\Lambda r}), \quad (10)$$

$$v_{2\pi}^A = \sqrt{2}\pi \frac{h_\pi^1}{\Lambda^3} \{g_A L^A(r) - g_A^3 [3L^A(r) - H^A(r)]\} \quad (11)$$

with

$$L^A(r) = \frac{\Lambda^2}{8\pi r} \int_{4m_\pi^2}^{\infty} \frac{dt'}{\sqrt{t'}} \sqrt{t' - 4m_\pi^2} \\ \times \left( \frac{e^{-\sqrt{t'}r} - e^{-\Lambda r}}{\Lambda^2 - t'} - \frac{e^{-\Lambda r}}{t' - 4m_\pi^2} \right), \quad (12)$$

$$H^A(r) = \frac{m_\pi^2 \Lambda^2}{2\pi r} \int_{4m_\pi^2}^{\infty} \frac{dt'}{\sqrt{t'}} \frac{1}{\sqrt{t' - 4m_\pi^2}} \frac{e^{-\sqrt{t'}r} - e^{-\Lambda r}}{\Lambda^2 - t'} \quad (13)$$

## 2.2 Asymmetry in $np \rightarrow d\gamma$

The photon asymmetry in  $np \rightarrow d\gamma$ ,  $A_\gamma$ , is defined from the differential cross section of the process as

$$\frac{d\sigma}{d\Omega} \propto 1 + A_\gamma \cos\theta, \quad (14)$$

where  $\theta$  is the angle between the neutron polarization and the out-going photon momentum. Non-zero  $A_\gamma$  values arise from the interference of opposite parity transition amplitudes, *e.g.* M1 and E1.

At the thermal energy where the process occurs, lowest order EM operators may suffice, therefore we consider the E1 operator,

$$\mathbf{J}_{E1} = -i\frac{\omega_\gamma}{4} (\boldsymbol{\tau}_1^z - \boldsymbol{\tau}_2^z) \mathbf{r}, \quad (15)$$

where  $\omega_\gamma$  is the energy of out-going photon. At the leading order of  $h_\pi^1$ ,  $A_\gamma$  is proportional to  $h_\pi^1$ , and we can write  $A_\gamma$  as

$$A_\gamma = a_\gamma h_\pi^1, \quad (16)$$

with

$$a_\gamma = -2 \frac{\text{Re}(\mathcal{M}_1 \mathcal{E}_1^*)}{|\mathcal{M}_1|^2}, \quad (17)$$

where  $\mathcal{E}_1$  and  $\mathcal{M}_1$  are matrix elements of the E1 and M1 transitions, respectively. Analytic forms of these amplitudes can be found in [9].

## 3 Result

Fig. 2 shows  $v_{1\pi}^A(r)$  (eq. (10)) and  $v_{2\pi}^A(r)$  (eq. (11)) in the range  $0 < r < 5$  fm as functions of cutoff  $\Lambda$ . The curve denoted by ‘Yukawa’ in OPEP corresponds to an infinite cutoff value. In the long range region (right panels), both OPEP and TPEP seldom depend on  $\Lambda$ . The magnitude of TPEP in the long range is smaller than OPEP by an order of 10, which confirms the dominance of OPEP in the long-range region. In the short range, *e.g.*  $r < 1$  fm, substantial cutoff dependence is observed. The potential converges to the limiting case (infinite cutoff) with increasing  $\Lambda$ . The change due to the cutoff value is simple in OPEP, but TPEP shows more diversity in the dependence on the cutoff. TPEP is a decreasing function at small  $r$  but the sign of the curvature changes at a certain value of  $r$  and then it becomes increasing. The value of  $r$  at which the

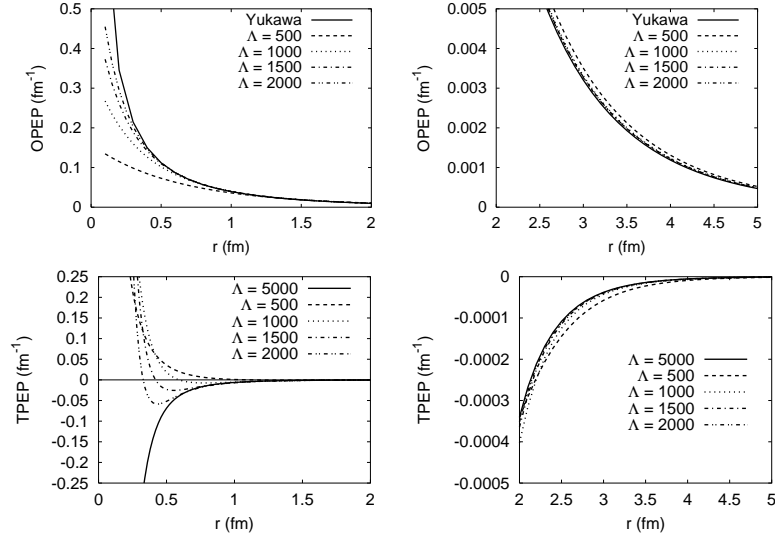


**Fig. 2.**  $v_{1\pi}^A(r)$  (upper row) and  $v_{2\pi}^A(r)$  (lower row) in the short-intermediate (left column) and long (right column) ranges.

**Table 1.** OPE and TPE contributions to the asymmetry as functions of cutoff  $\Lambda$ .

| $\Lambda$ (MeV)  | 500     | 1000    | 1500    | 2000    |
|------------------|---------|---------|---------|---------|
| $a_\gamma$ (OPE) | -0.1074 | -0.1125 | -0.1126 | -0.1124 |
| $a_\gamma$ (TPE) | -0.0022 | 0.0073  | 0.0117  | 0.0133  |

curvature of TPEP becomes zero is sensitive to  $\Lambda$ , and it gives significant effect to  $a_\gamma$ .

In Table 1, we show the numerical result of  $a_\gamma$  defined in eq. (16). With OPEP,  $a_\gamma$  is stable against the variation of the cutoff value, and there is about 5% fluctuation at most with the cutoff values considered in the present work. The TPEP contribution to  $a_\gamma$ , on the other hand, varies significantly in magnitude and even sign change occurs. From the behavior of  $v_{1\pi}^A(r)$  and its contribution to  $a_\gamma$ , it can be deduced that a decreasing function gives negative contribution to  $a_\gamma$ . With a larger  $\Lambda$ , the value of  $r$  at which  $\partial_r v_{2\pi}^A(r) = 0$  becomes smaller, and the decreasing region of  $v_{2\pi}^A(r)$  gets narrower. This means that the negative contribution becomes smaller in magnitude and a more positive contribution comes from TPEP. This explains well the sign and magnitude behavior of  $a_\gamma$  with TPEP.

## 4 Summary

We have calculated the PV TPE  $NN$  potential from the EFT, and applied it to the calculation of PV asymmetry in  $np \rightarrow d\gamma$  at threshold. In the intermediate and long range region, TPEP is smaller than OPEP by an order of magnitude. TPEP is comparable to OPEP for  $r < 0.5$  fm. Sizable cutoff dependence of the potential appears at  $r \leq 1$  fm for both OPEP and TPEP. The asymmetry also shows

non-negligible cutoff dependence. For the asymmetry with OPEP, the dependence is relatively weak and the result shows convergent behavior with larger cutoff values. On the contrary, the asymmetry with TPEP is strongly dependent on the cutoff value, even accompanied by a sign change, and the convergence of the result is not clearly seen. As a result, the TPEP contribution to the asymmetry is about  $-2\% \sim 12\%$  of the OPEP in the cutoff range 500  $\sim$  2000 MeV. Since 2000 MeV is a sufficiently large cutoff value, the contribution of TPEP, though uncertain, lies in the range of (a few  $\sim 10\%$ ) of OPEP. This is a significant correction to the OPEP result compared to one-heavy-meson exchange, which is less than 1% of OPEP [9], but it is good to justify that the perturbative expansion of EFT works well for the PV  $NN$  potential. The low energy constant terms at the NNLO, which are not considered in this work, could give a similar amount of correction.

## References

1. B. Desplanques, J. F. Donoghue and B. R. Holstein, Ann. Phys. (N.Y.) **124**, 449 (1980).
2. B. Desplanques, Phys. Lett. **41B**, 461 (1972).
3. H. J. Pirner and D. O. Riska, Phys. Lett. **B 44**, 151 (1973).
4. M. Chemtob and B. Desplanques, Nucl. Phys. **B 78**, 139 (1974).
5. S.-L. Zhu, C. M. Maekawa, B. R. Holstein, M. J. Ramsey-Musolf and U. van Kolck, Nucl. Phys. **A 748**, 435 (2005).
6. B. Desplanques, Phys. Lett. **B 512**, 305 (2001).
7. C. H. Hyun, T.-S. Park and D.-P. Min, Phys. Lett. **B 516**, 321 (2001).
8. R. Schiavilla, J. Carlson and M. W. Paris, Phys. Rev. C **70**, 044007 (2004); *ibid* **67**, 032501(R) (2003).
9. C. H. Hyun, S. J. Lee, J. Haidenbauer and S. W. Hong, Eur. Phys. J. **A 24**, 129 (2005).
10. B. Desplanques, Phys. Rep. **297**, 1 (1998).
11. C. H. Hyun, S. Ando and B. Desplanques, in preparation.

